Malaysian Journal of Civil Engineering 27 Special Issue (1):178-194 (2015)

LONG-TERM RESPONSE PREDICTION OF INTEGRAL ABUTMENT BRIDGE UNDER TIME-DEPENDENT EFFECT

Akilu Muhammad*, Redzuan Abdullah & Moh'd Salleh Yassin

Faculty of Civil Engineering, UniversitiTeknologi Malaysia, 81310 Skudai, Johor Bahru, Malaysia

*Corresponding Author: *akilmuh@yahoo.com*

Abstract: Parametric study was conducted to assess the time-dependent effect of creep on long-term behaviour of prestressed concrete Integral Abutment Bridge (IAB). Varying backfill soil types (dense sand, loose sand, stiff clay, soft clay) were provided behind the bridge abutment and the interaction was modelled using linear springs. The effect of backfill soil type on the behaviour of the bridge was assessed through 75-year time-history numerical simulations using Finite Element Method. CEB-FIP 1990 creep model was used to analyse the linear viscoelastic behaviour of creep. The result of the long-term response prediction showed significant increase in bridge displacement due to creep. Displacement due to creep was found to be nearly five times displacement due to instantaneous loading and abutment bending moment increased by more than two times that of live and dead loads. There is marked difference in girder and abutment shears, abutment axial load and abutment moment as a result of variation of backfill soil. The Denser the backfill soil the lesser the magnitude of the reactions on the bridge abutment and girder indicating a favourable choice of compacted sandy soil behind integral bridge abutments.

Keywords: *Creep, integral abutment bridge, soil-structure interaction, finite element method*

1.0 Introduction

Integral Abutment Bridges (IABs) or Jointless bridges are bridges constructed without conventional expansion joints and bearings, their superstructure and abutment are rigidly connected. IABs have recently become popular among Bridge Engineers due to their economic advantage. Expensive repair and replacement works that usually consume a huge amount of bridge maintenance budget are carried out to repair faulty joints and bearings (Wolde-Tinsae *et al.*, 1988; Vasant, 2005; Sophia *et al.*, 2006). Leaking joints account for 70% of defects occurring at ends of girder, piers and abutment seats (Rodolf *et al.*, 2005). Absence of joints in IABs resulted in significant savings in bridge maintenance budget. It adds to the redundancy of the structure thereby improving its structural performance especially during seismic loading.

Despite these advantages, there are concerns that creep and temperature loading may lead serviceability problems that can result to inadequate long-term performance of IABs. Paucity of design codes for IABs has resulted in numerous research works on its long-term performance under temperature and time-dependent loads.

Concrete Creep was discovered to have adverse effect on IAB response and long-term behaviour (Kim and Laman 2010), it causes changes in rheological and material properties leading to strain development in concrete structure Debbarma and Saha (2011). Deflection due to time-dependent loading was found to be equal to the deflection from instantaneous loading (Arockiasamy and Savikumar, 2005). Pugasap *et al.* (2009) discovered that Creep and Shrinkage led to long term top abutment displacement while bottom abutment displacement was due to time dependent effects and elastoplastic behaviour.

In many of these research works, soil-structure interaction was identified as a major factor affecting the bridge behaviour (Huang *et al.*. 2008, Dicleli and Erhan 2009, Kalayci *et al.*. 2009, Noorzaei *et al.*. 2010). For instance, it was discovered that the denser the backfill of sandy soil the more the axial forces and moments on the bridge deck (Faraji *et al.*, 2001). Pile moments were found to be minimized with denser backfill and lower pile restraint (Civjan and Bonczar, 2007).

Fewer research works were conducted on the effect of creep on IABs under varying types of backfill. Since previous research works have established the importance soil-structure interaction on the behaviour of IABs, there is the need to understand the response of IABs to different types of backfill under creep effect. In this research, a parametric study was undertaken on 75-year behaviour of long span prestressed concrete girder IAB under creep effect using finite element software, LUSAS.

2.0 The Bridge Details

The bridge is a 210m long concrete slab on prestressed concrete girder IAB (Figure 1). It has seven equal Pier-to-Pier spans of 30m length (Figure 2a) and 11 equally spaced standard prestressed concrete T-beams of 2.7m depth (Figure 2c) with longitudinal length of 30m provided along the 13.9m bridge width to support 20mm thick Deck Slab. The bridge has two carriage ways of 3.65m on each of its two lanes. The girders were seated on pier caps placed transversely at 30m intervals and the pier caps were supported by three piers (Figure 1). At each end of the bridge, the longitudinal beams were embedded into 1.2m thick and 6m high abutments (Figure 2b). Abutments were supported by a pile cap sitting on 21 closely spaced 0.6 m diameter circular Piles. The whole structure acts like a single frame system with rigid connection between the superstructure and the substructure. The bridge is horizontal without skew or curvature.

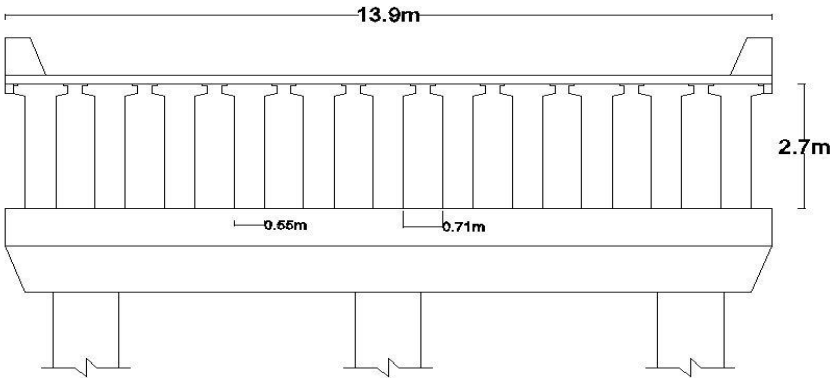

Figure 1: Section of the superstructure of the Integral Bridge.

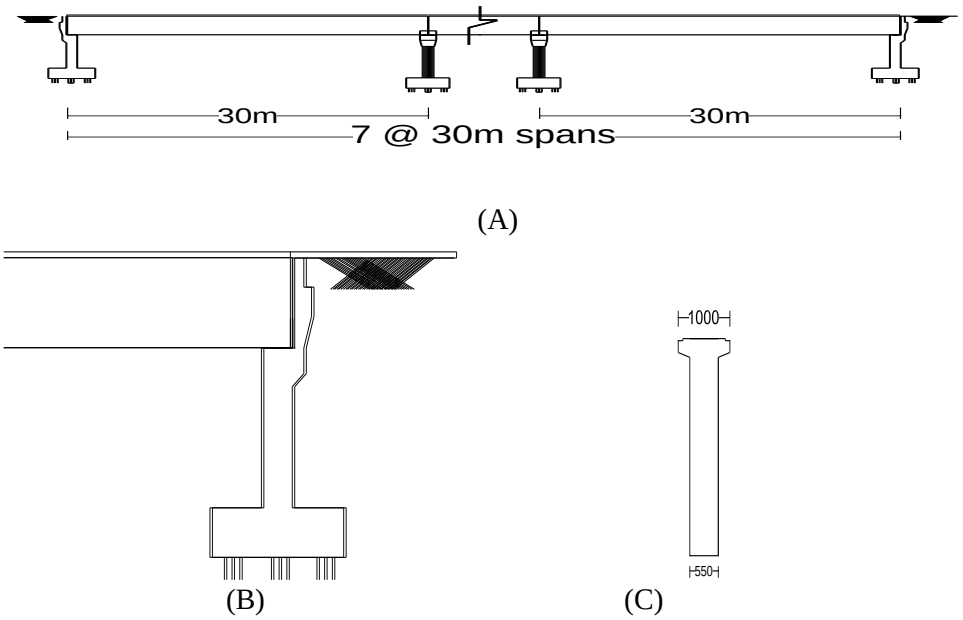

Figure 2: (A) Elevation of the 210m long bridge. (B) Girder abutment integral connection. (C) Posttensioned T-beam (Dimensions in mm).

The bridge girders were designed as continuous Post tensioned concrete T beams. prestress force of 4600 KN was applied on both sides of the girder using 7 wire standard strand of 12.9mm diameter and 195E6 kN/m^2 Modulus of Elasticity. Secondary moments from prestress cable were analysed using equivalent load method in Prab (2011) and calculated using the equation:

$$q = 8x(e3 - \left(\frac{e1+e2}{2}\right)x\left(\frac{p}{l^2}\right) \quad (1)$$

Where q is the equivalent load from cable, *p* is prestress force and *x* is the cable curvature, *L* is the length of a beam, *e1*, *e3* and *e2* are the prestress cable eccentricities at left-end, mid- span and right-end of the beam respectively.

3.0 Finite Element Model

A longitudinal strip of the bridge comprising of four beams resting on Pier cap which supported by Pier and Pile cap was used to idealise the bridge model (Figure 3). BTS3 element in LUSAS, a three-dimensional thick non-linear beam element with linear interpolation and having CEB-FIP1990 creep material properties was used to model post-tensioned concrete T-girders. BMS3 element in LUSAS, a three dimensional thick beam element with linear interpolation was used to model abutment wall, pier, pier head, and pile head. Line meshing was applied to entire structural elements of the bridge.

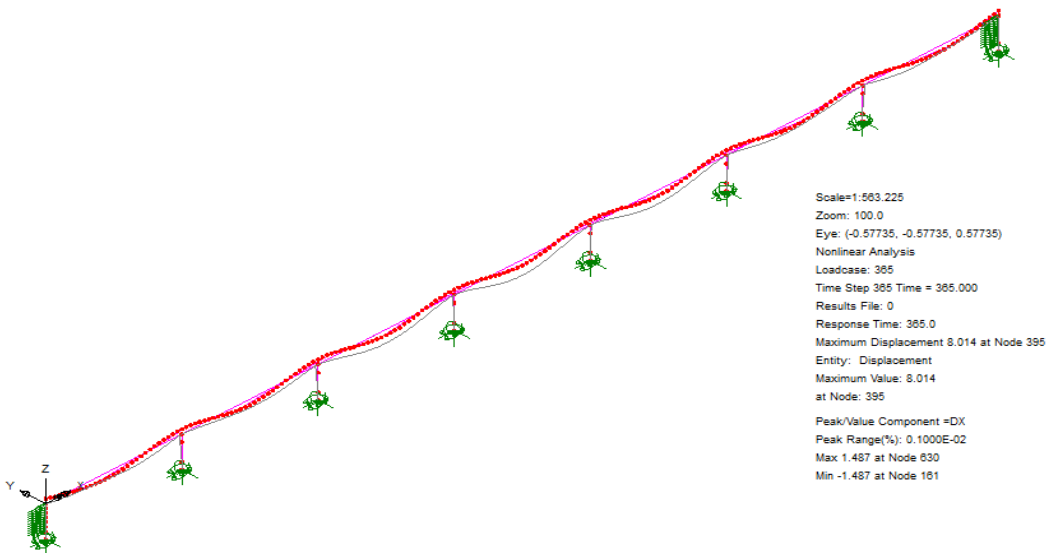

Figure 3: Finite Element model of the Bridge.

Tables 3 and 4 provides the geometric and materials properties of the bridge members. CEB-FIP 1990 concrete creep model was used in modelling the material properties of concrete girder for creep analysis. The remaining structural elements were modelled using material properties of BS 5400 concrete grade 40. Prestress force on girder was

modelled using line mesh (Figure 4). Horizontal line represents the beam while curved line represents tendon. Both the beam and the tendon are modelled as beam element. Single tendon prestress wizard in LUSAS calculates equivalent prestressing force from tendon and applies it to beam at nodal points. This creates the prestressing effect of tendon on the beam.

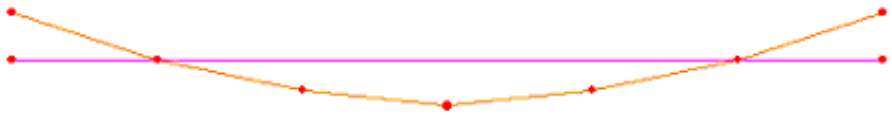

Figure 4: Beam and Tendon model.

The bridge loading comes from its self-weight and imposed load. Imposed load comprised of HA- UDL, HA-KEL and HA-HB 45 loads according to BD37/01 design manual of roads and bridges (British Highway Agency, 2001). Different load cases were considered for the superstructure live and dead loads and the load case that gave the worst loading condition was used in the analysis.

Table1: Prestress definition to BS5400

Tendon Details		Short-term loss		Long-term loss	
Prestressing force	9.2E6 N	Duct friction coefficient	0.55	Relaxation loss	2.5%
Modulus of Elasticity	195E6 kN/m^2	Wobble factor	3.3E-3 /m	Shrinkage coefficient	0.2E-3
Tendon Area	5.7E3 mm^2			Creep coefficient	0.036E-6 m^2/kN
End Slip	5E-3mm each end			Stress at transfer	15E3 kN/m^2
Jacking	Both ends				

Table 2: Geometric property of Bridge members.

Member	Area (mm^2)	Second moment of are about yy axis (mm^4)	Second moment of are about zz axis (mm^4)	Product moment of area lyz	Torsional constant Jxx
T-beam	1.81635E6	1.58525E12	54.8328E9	-93.2915E6	148.969E9
Abutment	10.2915E12	62.8587E24	1.03049E24	-4.40733E21	3.85918E24
Pier head	3.04E6	793.085E9	733.419E9	-24.0138E6	1.31989E12
Pier	6.24E6	14.0255E12	715.892E9	-0.585938	2.44947E12
Pile head	8.16E6	1.92567E12	15.6284E12	670.41E6	5.98345E12

Table 3: Material Properties of bridge girders.

Material	Yong Modulus Nmm	Poisson's ratio	Mass density N/mm^3	Coefficient of thermal expansion	Mean compressive strength N/mm^2	Relative humidity %	Nominal size mm
BS5400 Concrete creep CEB-FIP	28E3	0.2	2.4E-9	0.012E-3	50	70	462.6
BS 5400	28E3	0.2	2.4E-9	0.01E-3	50	70	462.6

4.0 Creep Calculation

Concrete undergo physical and chemical change in volume as a result of its interaction with the environment. Time-dependent deformations in concrete like creep, shrinkage and relaxation are as a result of the hydration process of concrete as it interacts with the environment over time. These deformations need to be considered in the study of long-term behaviour of concrete. In this research, Time-history response prediction was carried out to analyse the effect of creep on the performance of long span IAB over a 75 year period, in line with American State Highway and Transportation Officials (ASHTO) prescribed bridge life span period of 75 years. The nonlinear viscous behaviour of creep in concrete was analysed using CEB-FIP 1990 creep model and Modified Newton Raphson method was used for the nonlinear iteration. CEB-FIP

Model Code 1990 calculates the total strain in a concrete member that is uniaxially loaded at time t_0 with a constant stress $\sigma_c(t_0)$, as follows:

$$\varepsilon(t_0) = \varepsilon_{ci}(t_0) + \varepsilon_{cc}(t) + \varepsilon_{cs}(t) + \varepsilon_{cT}(t) \tag{2}$$

$$= \varepsilon_{c\sigma}(t) + \varepsilon_{cn}(t) \tag{3}$$

Where;

$\varepsilon_{ci}(t_0)$ is the initial strain at loading.

$\varepsilon_{cc}(t)$ is the creep strain at time $t > t_0$

$\varepsilon_{cs}(t)$ is the shrinkage strain.

$\varepsilon_{cT}(t)$ is the thermal strain.

$\varepsilon_{c\sigma}(t)$ is the stress dependent strain: $\varepsilon_{c\sigma}(t_0) = \varepsilon_{ci}(t_0) + \varepsilon_{cc}(t)$

$\varepsilon_{cn}(t)$ is the stress independent strain: $\varepsilon_{cn}(t_0) = \varepsilon_{cs}(t_0) + \varepsilon_{cT}(t)$

Creep is assumed to have a linear relationship with stress within the range of service stress. For a constant stress at time t_0 , creep strain is obtained as:

$$\varepsilon_c(t) = \frac{\sigma_c(t_0)}{E_c(t_0)}[1 + \varphi(t, t_0)] \tag{4}$$

Where, $\varphi(t, t_0)$ is creep coefficient which is a ratio of creep to instantaneous strain and E_c is Modulus of Elasticity in 28 days.

The stress dependent strain, $\varepsilon_{c\sigma}(t, t_0)$, may then be expressed as:

$$\varepsilon_{c\sigma}(t, t_0) = \sigma_c(t_0)[\frac{1}{E_c(t_0)} + \frac{\phi(t, t_0)}{E_{ci}}] = \sigma_c(t_0) J(t, t_0) \tag{5}$$

Where, $J(t, t_0)$ is the creep function, $E_c(t_0)$ is the modulus of elasticity at the time of loading t_0 and $\frac{1}{E_c(t_0)}$ represents the initial strain per unit stress at loading.

The principle of superposition is assumed to be valid for variable stresses or strains. It is used to obtain the constitutive equation for concrete creep also known as integral type creep law as expressed in equation (6).

$$\varepsilon_c(t) = \sigma(t_0)J(t,t_0) + \int_{t_0}^{t} J(t,\tau)\frac{\partial\sigma_c(\tau)}{\partial\tau}\partial\tau + \varepsilon_{cn}(t) \quad (6)$$

Notional creep coefficient is estimated from the equation below:

$$\varphi(t,t_0) = \varphi_0\beta_c(t-t_0) \quad (7)$$

φ_0 is the notional creep coefficient.

β_c is the coefficient to describe the development of creep with time after loading.

t is the age of concrete (days) at the moment considered.

t_0 is the age of concrete at loading (days).

In the CEB-FIP Code the notional creep coefficient is calculated from

$$\varphi_0 = \varphi_{RH}\beta(f_{cm})\beta(t_0) \quad (8)$$

With

$$\varphi_{RH} = 1 + \frac{1 - RH/RH_0}{0.46(h/h_0)^{1/3}} \quad (9)$$

$$\beta(f_{cm}) = \frac{5.3}{(f_{cm}/f_{cm0})^{0.5}} \quad (10)$$

$$\beta(t_0) = \frac{1}{0.1 + (t_0/t_1)^{0.2}} \quad (11)$$

Where;

h is the notional size of the member (mm) = $2Ac/u$, Ac is area of cross section, *u* is length of the perimeter of the cross section which is in contact with the atmosphere. f_{cm} is the mean concrete compressive strength (MPa) at 28 days. f_{cmo} = 10MPa, *RH* is the relative humidity of the ambient environment (%), RH_0 = 100% and h_0 = 100mm (Comite Euro-International du Beton, 1990). The development of creep with time is given by

$$\beta_c(t-t_0)=\left[\frac{(t-t_0)/t_1}{\beta_H+(t-t_0)/t_1}\right]^{0.3} \tag{12}$$

With

$$\beta_H=150\left\{1+\left(1.2\frac{RH}{RH_0}\right)^{18}\right\}\frac{h}{h_0}+250\le 1500 \tag{13}$$

5.0 Soil-Structure Interaction

Due to the rigid connection between the superstructure and the abutment, backfill-abutment interaction and pile-soil interaction becomes the only means of accommodation of longitudinal movement from live loads, creep and shrinkage. The soil-structure interaction becomes an important factor in the behaviour of IABs. Because piles and the pile caps are buried in the soil, the horizontal load on the group of piles can be resisted by the friction and passive soil resistance (Prab *et al.*, 2006), pile members were therefore not considered in the model. A series of Winkler springs support were used to approximate backfill soil behavior. This is sufficient because the concern this research is on structural behavior of the bridge and not soil movement that may necessitate a continuum model. The horizontal spring stiffness per square meter of the backfill of stiffness E_s behind abutment of depth H and transverse length L is approximated in equation (14) (O'Brien *et al.*, 2005).

$$k_{horz}=\frac{(4/\pi)E_S}{(L/H)^{0.6}H}\,KN/m/m^2 \tag{14}$$

E_s was approximated by Lehane *et al.* (1996) to be:

$$E_s=150000\frac{(2.17-e)^2}{(1+e)}\left(\frac{p'}{p_{atm}}\right)^{0.5}\left(\frac{0.0001}{\gamma}\right)^{0.4}KN/m^2 \tag{15}$$

Dry density of soil ρ_d, used in specifying the degree of compaction of backfill, is related to the void ratio in equation (16) which is used in obtaining void ratio of soil.

$$\rho_d = \frac{G_s \rho_w}{(1+e)} \tag{16}$$

Where G_s and ρ_w are the specific gravity of soil and density of water respectively, e is the void ratio of soil, P' is the mean confining stress less pore water pressure in the soil, P_{atm} the atmospheric pressure (100kN/m^2), γ is the shear strain taken to have a range of 50x10^{-6} to 0.01. Properties of the backfill soil types used in the analysis are as shown in Table 4.

Table 4: Varying soil properties used in the Model (Michael (2001) and Bowles (1996)).

Soil type	Density (wet) kN/m^3	Void ratio of soil (*e*)	Average shear strain (γ) m	Soil Stiffness kN/m^2	Horizontal Spring Stiffness kN/m/m^2
Dense sandy soil	22	1.0	0.0002	375771.8	6991.4
Loose sandy soil	16	1.38	0.0002	186562.6	2695.9
Medium Stiff clay	18	1.23	0.0018	31728.2	4112.1
Soft clay	15	1.47	0.0002	15788.7	2024.9

6.0 Result and Discussion

From the result of the long-term response prediction of the IAB, the first ten years showed rapid increase in girder and abutment deformations (moment, shears, and deflections); more than half of the deformations were recorded in the first ten years. This is due to the effect of shrinkage and instantaneous strains in addition to creep strain that are experienced in the early age of concrete as discussed by Raymond and Gilbert (2011). The linearity of instantaneous strain is observed in the early ages of the deformations before the nonlinear creep behaviour came into effect (Figure 5-12).
Marked increase in girder displacement due to creep was observed. Girder deflection as a result of creep was found to exceed girder deflection from to live and dead loads by nearly five times (Figure 6). This finding follows the line of the findings of Arockiasamy and Savikumar, (2005) on composite IAB. They discovered deflection due to time-dependent loading to be equal to the deflection from instantaneous loading. The maximum value of Abutment bending moment caused by creep was also found to be more than twice the magnitude obtained from instantaneous loading (Figure 8). There is

also marked difference in girder and abutment, displacement and shears, abutment axial load and abutment moment as a result of variation of backfill soil (Fig 5-7, 9, 10-13). Denser backfill creates more restraint to abutment movement due to creep effects; this reduces the magnitude of the reactions on the bridge abutment and girder. Compacted sandy soil is a favourable choice for backfill of long span integral bridge abutments.
It can be seen that there is no significant difference in the bending moment of girder (Figure 7), girder axial load (Figure 10) due to variation of backfill soil.

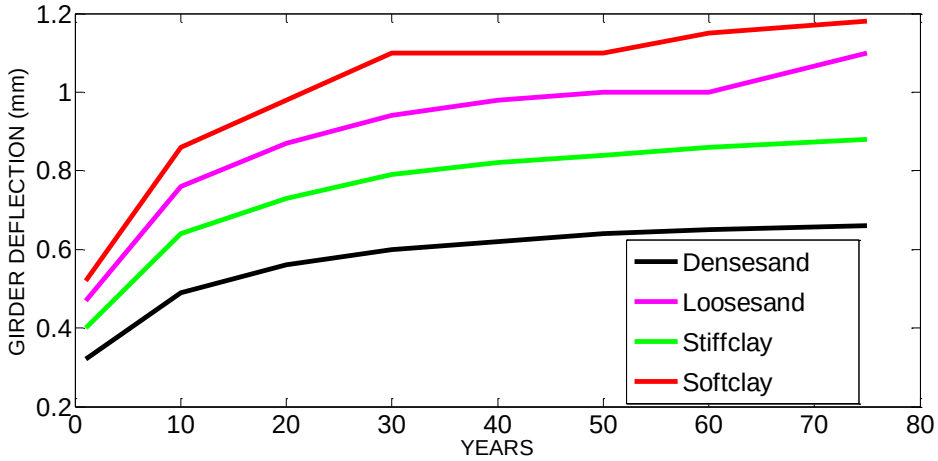

Figure 5: Variation of mid span Girder Displacement in 75 years under varying soil conditions.

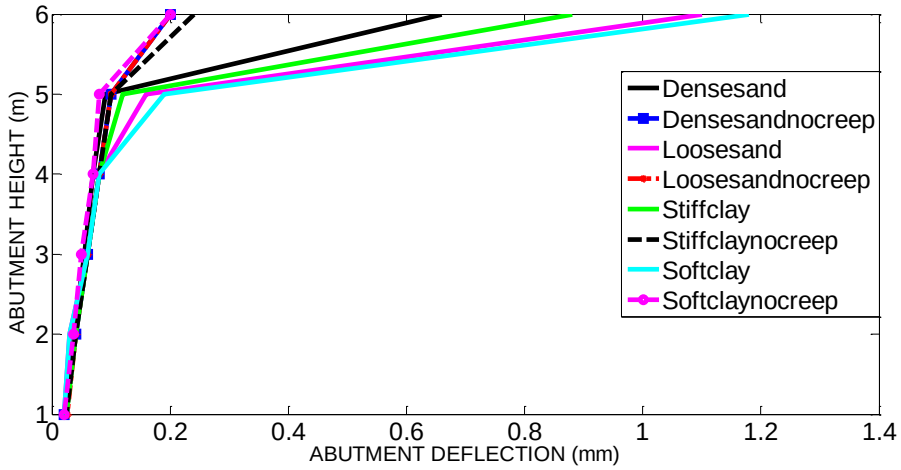

Figure 6: Variation of Abutment Displacement after 75 years under varying soil conditions.

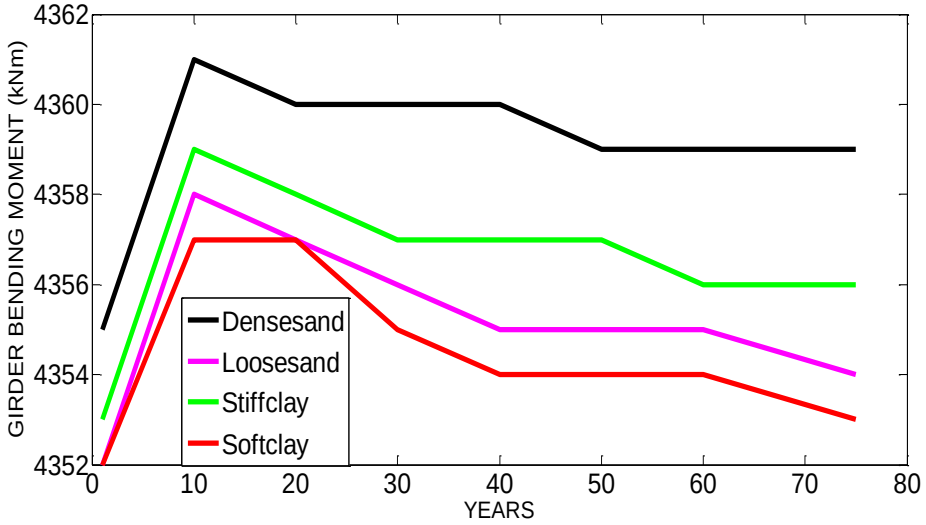

Figure 7: Variation Girder bending moment measures at mid span under varying soil conditions.

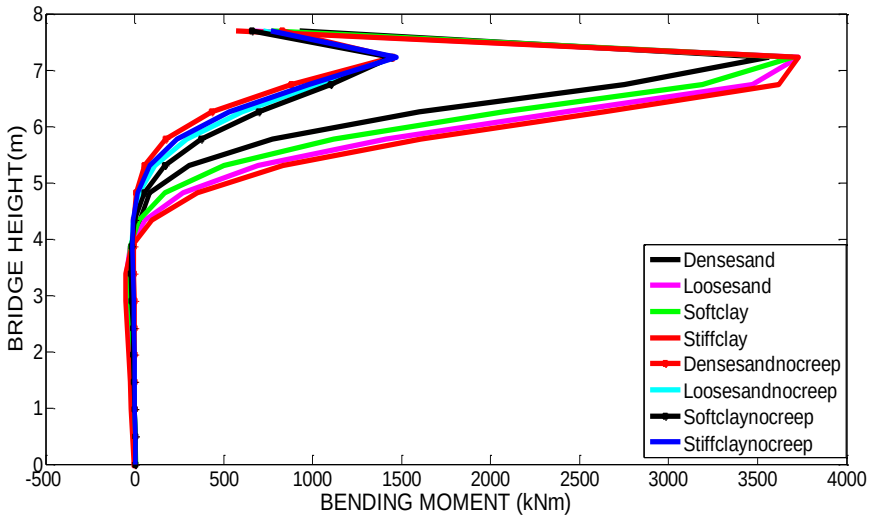

Figure 8: Abutment Bending Moment after 75years.

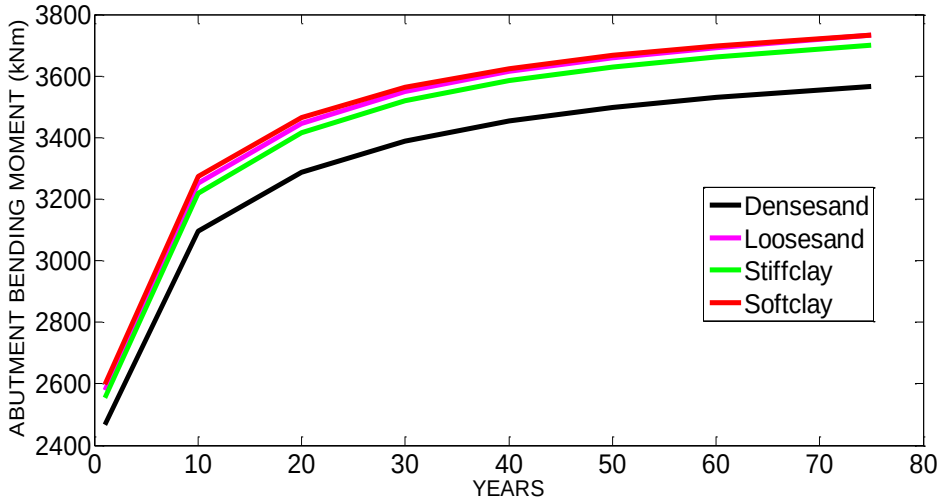

Figure 9: Variation of Abutment bending moment in 75years under varying soil conditions.

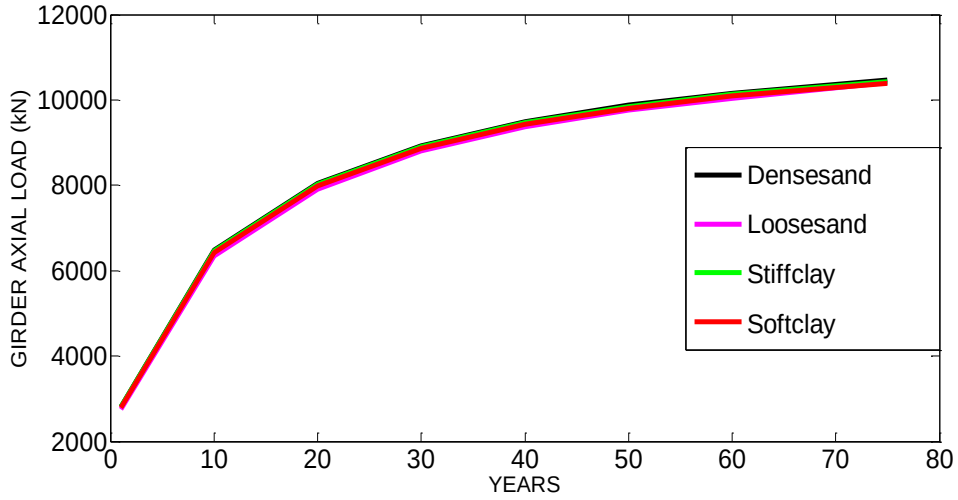

Figure 10: Variation of Girder axial load in 75years under varying soil conditions.

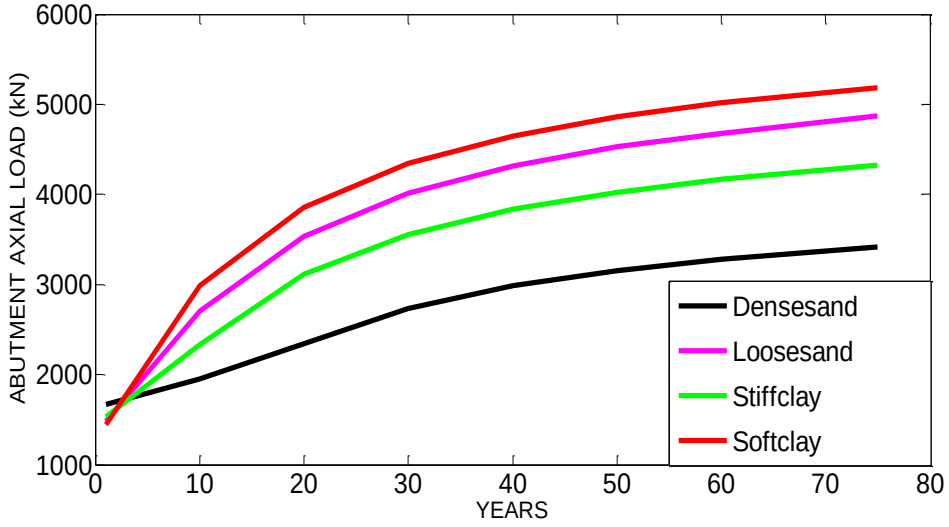

Figure 11: Variation of Abutment axial load in 75years under varying soil conditions.

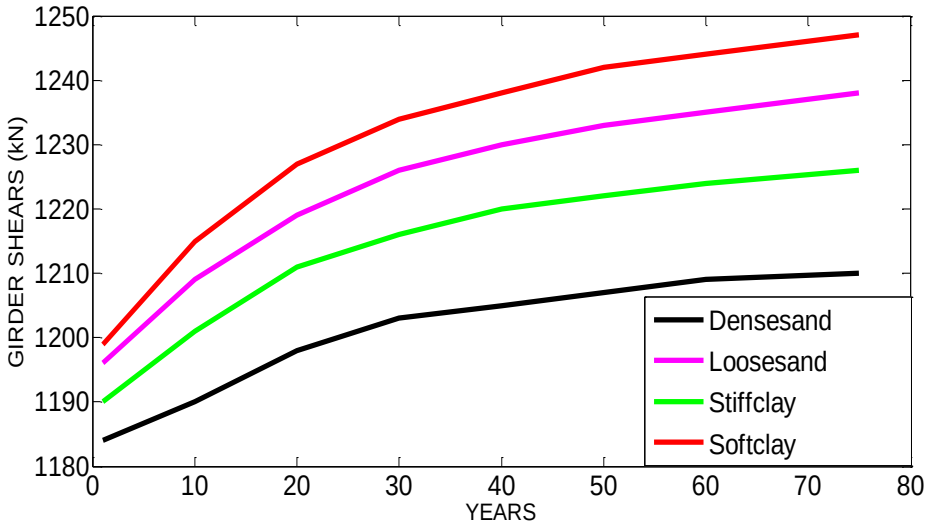

Figure 12: Variation of Girder Shears in 75years under varying soil conditions.

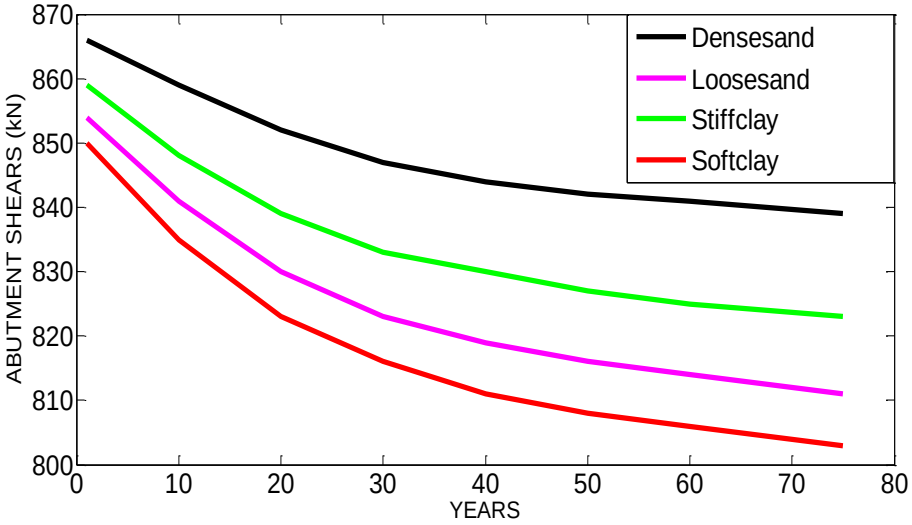

Figure 13: Variation of Abutment shears in 75years under varying soil conditions.

7.0 Conclusion

In conclusion, the research investigated the effect of creep on long-term behaviour of Integral Abutment Bridge under varying backfill soil. The research discovered significant effect of creep on the bridge performance, deformations due to creep were found to be more than twice the deformations obtained from instantaneous loading. Displacement due to creep was found to be nearly five times displacement due to instantaneous loading and abutment bending moment increased by more than two times the deformation obtained from live and dead loads. The effect of creep should be taken into account in structural designs of IABs.

There is marked difference in girder and abutment shears, abutment axial load and abutment moment as a result of variation of backfill soil. There is marked difference in girder and abutment shears, abutment axial load and abutment moment as a result of variation of backfill soil. The Denser the backfill soil the lesser the magnitude of the reactions on the bridge abutment and girder indicating compacted sandy soil is a good backfill behind integral bridge abutments.

References

Arockiasamy, M., Sivakumar. M. (2005). *Time-Dependent Behaviour of Composite Integral Abutment Bridges.* Practice Periodical of Structural Design and Construction Volume 10 No.3,

Bowles, J.E (1996) *Foundation Analysis and Design*, Fifth Edition, Mcgraw-Hill, New York,

British Highway Authority (2001) *Design Manual for Roads and Bridges*

British Standards Institute (1990) BS 5400-4:1990 Steel, concrete and composite bridges -Part 4: Code of practice for design of concrete bridges

Civjan, S. A., Bonczar, C., Brena, S. F., Dejong, J., & Crovo, D. (2007). *Integral abutment bridge behavior: Parametric analysis of a Massachusetts bridge*. Journal of Bridge Engineering, 12(1), 64-71.

Comite Euro-International du Beton, (1990) *CEB-FIP Model Code 1990,* Thomas Telford, Lausanne.

Debbarma, S.R., Saha, S. (2011) Behaviour of pre-stressed concrete bridge girders due to time dependent and temperature effects, First middle east conference on smart monitoring, assessment and rehabilitation of civil structures, Dubai.

Dicleli, M., & Erhan, S. (2009). *Live load distribution formulas for single-span prestressed concrete integral abutment bridge girders*. Journal of Bridge Engineering, 14(6), 472-486.

Faraji, S., Ting, J. M., Crovo, D. S., & Ernst, H. (2001). *Nonlinear analysis of integral bridges: Finite-element model.* Journal of Geotechnical and Geoenvironmental Engineering, 127(5), 454-461.

Huang, J., Shield, C. K., & French, C. E. W. (2008). *Parametric study of concrete integral abutment bridges*. Journal of Bridge Engineering, 13(5), 511-526.

Kalayci, E., Breña, S. F., & Civjan, S. A. (2009). Curved integral abutment bridges - thermal response predictions through finite element analysis.

Kim, W., & Laman, J. A. (2010). *Numerical analysis method for long-term behavior of integral abutment bridges*. [doi: 10.1016/j.engstruct.2010.03.027]. Engineering Structures, 32(8), 2247-2257.

Lehane, B., Keogh D. L. and O'Brien E. J (1996) *Soil-Structure interaction analysis for Integral Bridges* in Advances in Computational Methods for Simulation,(ed. B.H.V. Topping), Civil-Comp Press, Edinburgh, pp.201-10.

Michael, R. L. (2001) *Civil Engineering Reference Manual for the PE Exam*, 8th Edition, Professional Publications, Incorporated, Richmond US.

Noorzaei, J., Abdulrazeg, A. A., Jaafar, M. S., & Kohnehpooshi, O. (2010). *Non-linear analysis of an integral bridge*. Journal of Civil Engineering and Management, 16(3), 387-394.

O'Brien E. J., Keogh D. L., (2005). *Bridge Deck Analysis*., E & FN Spon, London.

Prab, B. (2011) *Prestressed Concrete Design to Eurocodes*, Routledge, New York.

Prab, B., Thomas, J., Ban, S. C. (2006) *Reinforced Concrete Design Theory and Examples*, Taylor and Francis, New York.

Pugasap, K., Kim, W., & Laman, J. A. (2009). *Long-term response prediction of integral abutment bridges*. Journal of Bridge Engineering, 14(2), 129-139.

Raymond I. G., & Ranzi, G. (2011). Time Dependent Behaviour of Concrete Structures New York: Spon Press.

Rodolfo, F., M., Samer H. P. (2005) *Integral Abutments and Jointless Bridges 2004 Survey Summary*, Proceedings of THE 2005 – FHWA on Conference Integral Abutment and Jointless Bridges organized by Constructed Facilities Center, College of Engineering and Mineral Resources, West Virginia University.

Sophia, H.,Yaser, K.,Eugenia, R.,Yousef, D., (2006) *Evaluation of Integral Abutment*, a research report, Department of Civil, Environmental and Ocean Engineering Stevens Institute of Technology Hoboken, N.J. 07030

Vasant C. (2005) *Integral Abutment and Jointless Bridges, proceedings of The 2005* – FHWA Conference, Constructed Facilities Centre College of Engineering and Mineral Resources, West Virginia University Baltimore, Maryland USA.

Wolde-Tinsae, Made, M. A., Klinger, J. E., and White, E. J. (1988). "*Performance of Jointless Bridges." Journal of Performance of Construction Facilities*, ASCE, Vol. 2, No. 2, pp. 111-125.